

DEADTIME CHARACTERISTICS OF ANGER CAMERAS

James A. Sorenson

University of Utah Medical Center, Salt Lake City, Utah

The deadtime characteristics of Anger cameras are analyzed from theoretical and experimental points of view. An investigation of two Searle Radiographics cameras revealed that they had both paralyzable and nonparalyzable components, the deadtimes of which varied with analyzer window width, the energy of the gamma rays counted, and the position of the "time constant selector" switch in the A-scope module of these cameras. A mathematical model for two-component systems is presented.

Considerable attention has been given to the question of Anger camera deadtime, and in particular to the model that best describes camera performance at high counting rates. Although some investigators (1,2) have assumed that the Anger camera behaves as a simple nonparalyzable system, others (3-5) have shown that most cameras behave as paralyzable systems or at least as if they have paralyzable components. For example, Arnold, et al (5) have shown that data from the Searle Radiographics Pho/Gamma III and HP cameras in their laboratory could be described under a variety of experimental conditions by a simple paralyzable model.

An additional possibility is that an Anger camera system might have both paralyzable and nonparalyzable components. As pointed out by Muehlechner, et al (4), the "front end" electronics of a Searle Radiographics camera (preceding the pulse-height analyzer) is a paralyzable system. Subsequent components, however, such as scalers or added data-processing hardware, are frequently nonparalyzable. Figure 1 shows such a system in schematic form. This model also is suggested by Budinger (6) who reported that the behavior of cameras in his laboratory was intermediate to that of the purely paralyzable and nonparalyzable models and is further supported by data obtained in our laboratory (7) to be discussed here.

For the system shown in Fig. 1, if $\tau_n \leq \tau_p$, the total system behavior follows that of the first component since the second component introduces no additional losses. The relationship between observed and true counting rates, R_o and R_t , is that of a simple paralyzable system and is given by (8):

$$R_o = R_t e^{-R_t \tau_p} \quad (1)$$

It can be shown that the deadtime, τ_p , is given by (8):

$$\tau_p = 1/R_t^{\max} \quad (2)$$

or:

$$\tau_p = 1/eR_o^{\max} \quad (3)$$

Received Aug. 9, 1974; original accepted Nov. 10, 1974.
For reprints contact: James A. Sorenson, Dept. of Radiology, University of Utah Medical Center, Salt Lake City, Utah 84132.

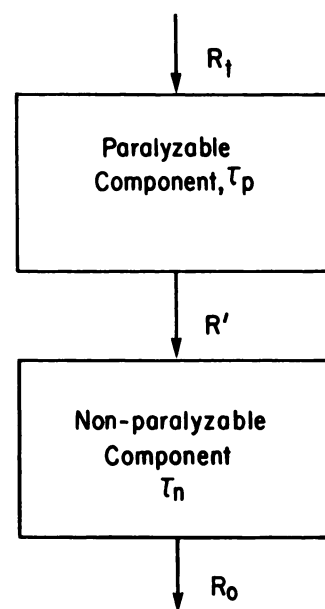


FIG. 1. Hypothetical counting system having paralyzable and nonparalyzable component in series.

where R_o^{\max} is the maximum observed counting rate and R_t^{\max} is the corresponding true counting rate. R_o^{\max} , and thus τ_p , can be determined with a single source by varying source-to-detector distance or by varying the source strength.

If $\tau_n > \tau_p$, the situation is more complicated. An approximate description of such a system is as follows:

$$R_o \approx R_t / \{e^{R_t \tau_p} + (k - 1)R_t \tau_p\} \quad (4)$$

where $k = (\tau_n / \tau_p)$.

The derivation of Eq. 4 is as follows: At the output of the first component (Fig. 1), the observed counting rate is:

$$R' = R_t e^{-R_t \tau_p} \quad (5)$$

which is also the input to the second component. Each event observed at the output of the second component introduces a deadtime, τ_n , but during the initial τ_p of this interval no additional input pulses to the second component can occur. Thus the second component behaves as a nonparalyzable system with input counting rate R' and effective deadtime $(\tau_n - \tau_p)$. Applying the appropriate equation for a nonparalyzable system (8), one obtains:

$$R_o \approx R' / \{1 + R'(\tau_n - \tau_p)\} \quad (6)$$

from which follows Eq. 4.

Equations 4 and 6 are only approximations since the equation relating observed and true counting rates for a nonparalyzable system (on which Eq. 6 is based) applies, strictly speaking, only to random input counting rates. R' is not random because pulses separated by short time intervals have been removed from the distribution. The approximation given by Eq. 4, however, describes the behavior of real Anger

cameras quite well (see Fig. 3) and therefore its use is thought to be justified.

The behavior of a two-component system having deadtimes $\tau_p = 10 \mu\text{sec}$ and $\tau_n = 20 \mu\text{sec}$ is shown in Fig. 2. For comparison, the behavior of a paralyzable system with deadtime $\tau_p = 10 \mu\text{sec}$ and a nonparalyzable system with deadtime $\tau_n = 20 \mu\text{sec}$ are also shown. At low counting rates, the two-component system behaves as if only the slower, nonparalyzable component were present whereas at higher counting rates the behavior is similar to that of the paralyzable component but a lower maximum observed counting rate is obtained.

The appropriate equations for calculating deadtime are also more complicated. One can show by differentiating Eq. 4 with respect to R_t that Eq. 2 is still valid but that R_o^{\max} is now given by:

$$R_o^{\max} = (1/\tau_p) \{1/(e + k - 1)\} \quad (7)$$

Thus Eq. 3 no longer applies. The deadtime of the nonparalyzable component is given by:

$$\tau_n = 1/R_t^{\max} + 1/R_o^{\max} - e/R_t^{\max} \quad (8)$$

which is obtained by combining Eqs. 2 and 7.

There is no easy way to distinguish between a simple paralyzable and a combined paralyzable/nonparalyzable system on the basis of observed counting rates alone. For both systems, there is a maximum observed counting rate which is followed by a decrease in observed counting rate with increasing source strength or true counting rate. One difference between the two models is in the ratio (R_t^{\max}/R_o^{\max}) . For a paralyzable system:

$$R_t^{\max}/R_o^{\max} = e \quad (9)$$

whereas for the two-component system:

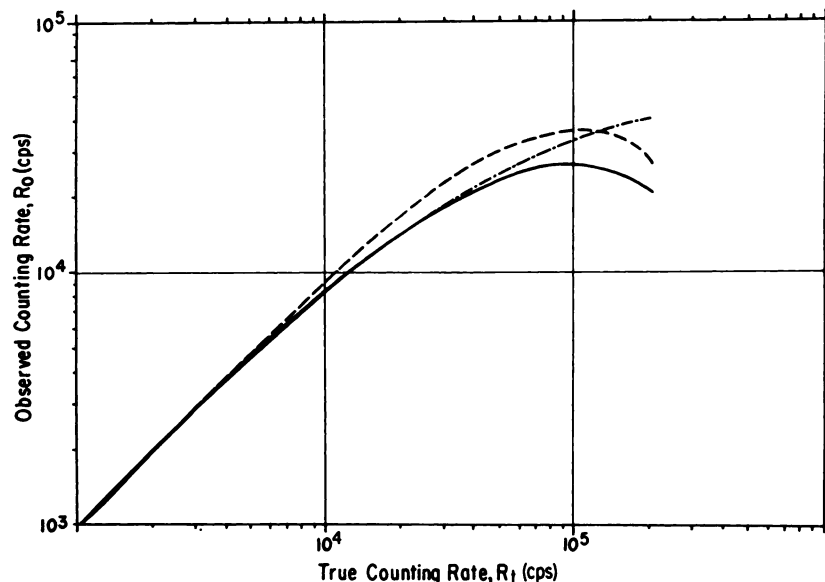


FIG. 2. Comparison of three counting systems: — paralyzable, $\tau_p = 10 \mu\text{sec}$; - - - nonparalyzable, $\tau_n = 20 \mu\text{sec}$; and — · — combined paralyzable/nonparalyzable, as in Fig. 1. $\tau_p = 10 \mu\text{sec}$, $\tau_n = 20 \mu\text{sec}$.

$$R_t^{\max}/R_o^{\max} > e \quad (10)$$

with the exact value depending on $k = (\tau_n/\tau_p)$. The ratio R_t^{\max}/R_o^{\max} can be determined experimentally by measuring R_o versus R_t over a range of counting rates about R_o^{\max} . Once R_o^{\max} and R_t^{\max} have been determined, then the deadtimes τ_n and τ_p of the two-component system can also be calculated using Eqs. 2 and 8. One method for accurately determining R_o versus R_t is described in the Methods section of this paper.

There are of course additional possibilities for multicomponent systems, for example, a system with two paralyzable components in series. The mathematical description of such a system represents a difficult problem that does not appear to have been solved in the literature. It also does not seem appropriate for Searle Radiographics cameras (7).

A series of experiments was carried out to determine the deadtime characteristics of two Searle Radiographics cameras. These were a Searle Radiographics Pho/Gamma III upgraded to HP status, hereafter denoted as Pho/Gamma III(HP), and a conventional Searle Radiographics HP camera. No auxiliary data-processing hardware was used in these experiments so the results reflect only the basic camera behavior.

EXPERIMENTAL METHODS

The relationship between R_o , the counting rate observed with the camera front panel scaler, and source activity A or true counting rate R_t , was determined under a variety of conditions for the Pho/Gamma III(HP) camera. The sources were placed on the floor for counting at a distance of about 1 meter from the uncollimated detector.

An accurate estimate of the true counting rate for each source used in an experiment was obtained as follows. All sources were first drawn up to the same total volume in syringes of the same size to avoid possible volume effects and then assayed for activity in a commercial dose calibrator (Squibb CRC6A). The same activity scale was used for all measurements to avoid possible scale change variations. A preliminary experiment revealed no significant nonlinearities ($<2\%$) over the range of dose calibrator response used. Then a counting measurement was carried out on the camera with the weakest source, which was of activity such that it was counted with less than 10% losses. Furthermore these losses were corrected using subsequent deadtime estimates. This measurement then provided a calibration factor of the true counting rate R_t versus activity A which could be applied to the other more active sources. Thus R_t was known for each source used in an ex-

periment with an estimated error of only a few percent.

Data were obtained on the Pho/Gamma III(HP) camera with ^{99m}Tc sources using different window widths (10, 20, and 35%) and a fixed base level (≈ 125 keV) and using a fixed window width (10%) but variable base level (125, 133, 137 keV). The effect of the position of the internal time-constant switch ("long" versus "short") in the A-scope module of this camera on ^{99m}Tc counting was also investigated. This switch is commonly in the "long" time-constant position when the camera is used with external data-processing hardware such as the "Data-Store" system and in the "short" position when it is used as a stand-alone imaging device. Additional experiments were carried out with ^{131}I sources using different window widths (10, 20, and 35%) and a fixed base level (≈ 330 keV). For the HP camera, only ^{99m}Tc was used with variable window widths and a fixed base level and with the internal time-constant switch in the "short" time-constant position only.

RESULTS

The two cameras evaluated in this study behaved under nearly all conditions analyzed as combined paralyzable/nonparalyzable systems. Figure 3 shows data obtained on the Pho/Gamma III(HP) camera for ^{99m}Tc counting with different window widths and a "short" time constant. Also shown are curves calculated from Eq. 1 or 4, using deadtimes calculated from Eqs. 2 and 8. The data and theoretical curves agree to within a few percent up to and slightly beyond R_t^{\max} . The same generally good agreement between data and theoretical curves was found under all conditions studied.

Table 1 summarizes ^{99m}Tc deadtimes for the two Searle Radiographics cameras as a function of window width and "time-constant" switch position. For both cameras, there was an apparent decrease in both the paralyzable and nonparalyzable deadtimes with increasing window width, with the paralyzable deadtimes showing the greatest variation. The deadtimes of the HP camera were all shorter than those of the Pho/Gamma III(HP) camera, especially in the paralyzable component. Switching from a "short" to a "long" time constant on the Pho/Gamma III(HP) camera significantly increased the nonparalyzable deadtime of the system but had little or no effect on the paralyzable component. Data from three experiments with the "long" time constant are presented to give an indication of the day-to-day variations in estimated deadtimes. They were typically 5% or less and may be attributed to day-to-day

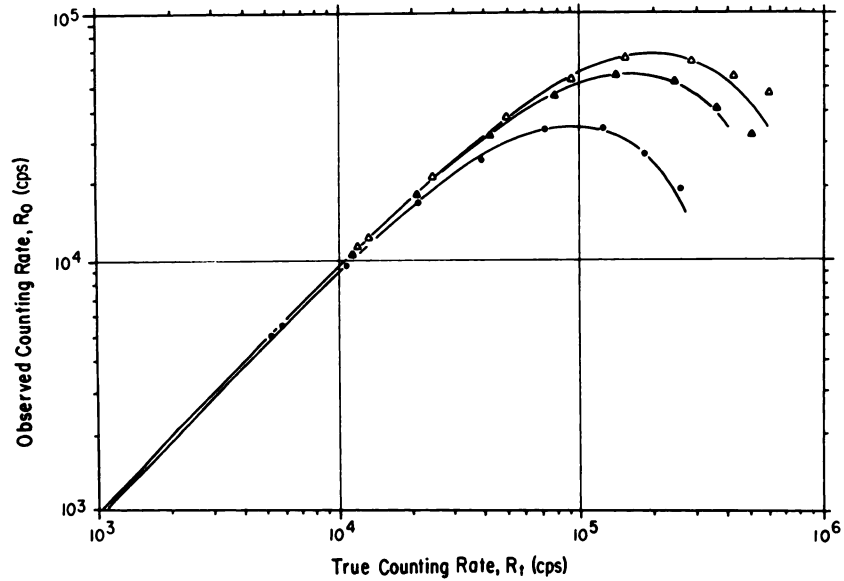


FIG. 3. Observed versus true counting rate for Pho/Gamma III (HP) camera and ^{99m}Tc. Solid lines calculated from Eq. 1 or 4, using deadtimes calculated from Eqs. 2 and 8. ● 10% window, $\tau_p = 10.5 \mu\text{sec}$; $\tau_n < \tau_p$. ▲ 20% window, $\tau_p = 5.9 \mu\text{sec}$; $\tau_n = 7.4 \mu\text{sec}$. △ 35% window, $\tau_p = 4.8 \mu\text{sec}$; $\tau_n = 6.2 \mu\text{sec}$.

TABLE 1. DEADTIMES (μsec) OF TWO SEARLE RADIOGRAPHICS CAMERAS (τ_p, τ_n)

| Nuclide | Camera | | | |
|---------------|-------------------|--------------------|--|------------------|
| | Standard HP | Pho/Gamma III (HP) | | |
| | ^{99m} Tc | ^{99m} Tc | ^{99m} Tc | ¹³¹ I |
| Time constant | Short | Short | Long† | Long |
| Window (%) | | | | |
| 10 | (9.0, 12.0) | (10.5, —)* | (10.9, 15.2) (10.8, 16.1) (11.1, 17.2) | (14.3, 28) |
| 20 | (4.3, 6.7) | (5.9, 7.4) | (5.9, 13.1) (5.9, 13.8) (5.9, 13.1) | (8.3, 20) |
| 35 | (3.6, 5.7) | (4.8, 6.2) | (5.0, 11.7) (4.8, 12.4) (5.0, 11.7) | (5.6, 11.3) |

* Dash indicates $\tau_n \leq \tau_p$.
† Measured on three different days.

experimental nonreproducibility, e.g., in the calibration of true counting rate versus source activity.

Only small variations were observed in the paralyzable and nonparalyzable deadtimes of the Pho/Gamma III(HP) camera when a fixed window width (10% or 14 keV) but variable base level was used for counting ^{99m}Tc. For example, data for 127- and 133-keV base levels indicated a two-component system with $\tau_p = 11 \mu\text{sec}$, $\tau_n = 15.2 \mu\text{sec}$ but data for a 137-keV base level were more accurately described by $\tau_p = 11 \mu\text{sec}$, $\tau_n = 16.5 \mu\text{sec}$.

The deadtimes of the Pho/Gamma III(HP) cam-

era were quite different for ¹³¹I versus ^{99m}Tc counting, being substantially longer for ¹³¹I. These data are also summarized in Table 1.

DISCUSSION

The Searle Radiographics cameras analyzed in this study behaved under most conditions as combined paralyzable/nonparalyzable systems rather than as simple paralyzable systems. These results are consistent with the observations of Budinger (6) but differ from those of Arnold, et al (5), who found that their Searle Radiographics cameras behaved under similar conditions as simple paralyzable systems. The reasons for these differences between apparently similar cameras are not clear. One valid conclusion, however, is that at least some Searle Radiographics cameras (and perhaps those of other manufacturers as well) behave as two-component rather than as simple paralyzable systems. Therefore they cannot be described accurately by a simple paralyzable model (Eq. 1) nor can their deadtimes be obtained by simple observations of R_o^{max} (Eq. 3). A detailed investigation of R_o versus R_t is required to establish the type of system that is involved and then to determine deadtimes.

Variations in deadtime observed under different experimental conditions in this work are consistent with the "window fraction" hypothesis of Muehleher, et al (4) and Arnold, et al (5). They propose a model in which each detected event produces a certain deadtime, the value of which is about 2 μsec for Searle Radiographics cameras (4). The observed losses for events falling within a certain analyzer window are therefore dependent on the number of events falling both inside and outside the window. Specifically, as the "window fraction" is decreased, relatively more events falling outside the window are

responsible for losses and the apparent deadtime for events falling within the window is increased.

This explanation is consistent with the data given for different window widths in Table 1. It also explains the difference between ^{99m}Tc and ^{131}I counting. Since ^{99m}Tc yields a larger photofraction, one expects for it a larger window fraction (for comparable photopeak windows) and consequently a shorter deadtime. The small variations seen with window centering are also consistent with this hypothesis since minor (5–10 keV) shifts about the photopeak have only small effects on the window fraction.

Because so many factors can influence measured deadtime, it is important that care be exercised when comparing deadtimes of different cameras. Although there are almost certainly real differences between different cameras, other factors that can have a significant effect on measured deadtimes include: (A) window setting; (B) nuclide counted; (C) scatter conditions; (D) position of internal switches in the camera; (E) deadtime of counting or data-processing hardware (e.g. scaler, computer, etc.); and (F) deadtime model assumed. Each of these factors must be considered before conclusions are drawn on the comparative deadtimes of different camera systems.

ACKNOWLEDGMENT

I am grateful to Gerald J. Hine, Veterans Administration, Washington, D.C., for helpful comments in the preparation of this paper.

REFERENCES

1. ADAMS R, ZIMMERMAN D: Methods for calculating the deadtime of Anger camera systems. *J Nucl Med* 14: 496–498, 1973
2. PAYNE JT, WILLIAMS LE, PONTO RA, et al: Comparison and performance of Anger cameras. *Radiology* 109: 381–386, 1973
3. ANGER HO: Testing the performance of scintillation cameras. *USAEC Report LBL-2027*, 1973, pp 1–7
4. MUEHLEHNER G, JASZCZAK RJ, BECK RN: The reduction of coincidence loss in radionuclide imaging cameras through the use of graded absorbers. *Phys Med Biol* 19: 504–510, 1974
5. ARNOLD JE, JOHNSTON AS, PINSKY SM: The influence of true counting rate and the photopeak fraction of detected events on Anger camera deadtime. *J Nucl Med* 15: 412–416, 1974
6. BUDINGER TF: High counting rate performance of the Anger scintillation camera. *USAEC Report LBL-2145*, 1973, p 4
7. SORENSON JA: Characterization of deadtime of Anger camera systems. *J Nucl Med* 15: 534–535, 1974
8. EVANS RD: *The Atomic Nucleus*, New York, McGraw-Hill, 1955, pp 785–788